Applied Catalysis B: Environmental 115–116 (2012) 74–80

Contents lists available at SciVerse ScienceDirect

Applied Catalysis B: Environmental

journal homepage: www.elsevier.com/locate/apcatb

Photo-chargeable and dischargeable TiO_2 and WO_3 heterojunction electrodes

Hyunwoong Park[a,*], Ayoung Bak[a], Tae Hwa Jeon[b], Seungdo Kim[c], Wonyong Choi[d]

[a] School of Energy Engineering, Kyungpook National University, Daegu 702-701, Republic of Korea
[b] Department of Energy Science, Kyungpook National University, Daegu 702-701, Republic of Korea
[c] Department of Environmental Science and Biotechnology, Hallym University, Chuncheon 200-702, Republic of Korea
[d] School of Environmental Science and Engineering, POSTECH, Pohang 790-784, Republic of Korea

ARTICLE INFO

Article history:
Received 6 October 2011
Received in revised form
21 November 2011
Accepted 3 December 2011
Available online 11 December 2011

Keywords:
Artificial photosynthesis
Discharging
Battery
Galvanic
Anticorrosion
Solar

ABSTRACT

TiO_2 and WO_3 heterojunction electrodes are studied for their bi-functionality on harvesting light and storing energy. Both semiconductors are fabricated either 'single' (mixed) electrodes or two different electrodes galvanically coupled in a mixed electrolyte of 0.1 M sodium formate and 0.1 M sodium chloride. Irradiation of AM 1.5-light shifts the open circuit potentials (OCPs) of the mixed and coupled electrodes from around −0.1 V_{SCE} (dark OCPs) to a potential range between −0.8 and −0.5 V_{SCE}, which slowly return to their respective dark OCPs over a period of around 14 h. Such discharging periods are significantly influenced by the irradiation (photocharging) time and weight or area ratios of TiO_2 and WO_3. When the TiO_2 and WO_3 mixed electrodes are galvanically coupled to stainless steel electrodes for application to anticorrosion, the mixed potentials of the couple are maintained at ca. −0.4 V_{SCE} over 10 h even after light off. The measured galvanic currents verify that the photogenerated electrons of TiO_2 flow to WO_3 (charging) and even overflow to the steel (cathodic protection) during the irradiation, while the stored electrons at WO_3 flow to the galvanically coupled steel electrodes directly or through the TiO_2 upon light off.

1. Introduction

Global energy demand is projected to continuously grow to around 50 TW in 2050 and over 100 TW in 2100 [1,2]. A variety of alternative energy sources are considered, and among them solar light is regarded the most viable to meet such a prodigiously large amount of energy demand. However, fluctuation of incident solar light resulting from climate, weather, locality, and diurnal variation requires its in situ or ex-situ storage for further use [3]. Interestingly, nature has already solved the problem by adopting a photosystem with bi-functionality through which solar light is harnessed, conversed, and simultaneously stored for the growth and reproduction of organism [4].

Recently, bio-inspired heterogeneous photocatalysts with such bi-functionality have received growing attention [5]. This approach can be achieved simply by coupling a light-harvesting (charging) material and a light-storing (discharging) material. For example, Tatsuma et al. demonstrated that a partial amount of electrons generated at UV-excited TiO_2 and WO_3 composite particles can be stored at WO_3 [6,7]. The electron storing mechanism of WO_3 is very similar to its electrochromism and photochromism (Eqs. (1)–(3))

$$e_{cb}^-(TiO_2) \rightarrow e_{cb}^-(WO_3)\ \text{(interfacial electron transfer)} \quad (1)$$

$$WO_3 + xe_{cb}^- + xH^+ \rightarrow H_xWO_3\ \text{(charging)} \quad (2)$$

$$H_xWO_3 \rightarrow WO_3 + xe_{cb}^- + xH^+\ \text{(discharging)} \quad (3)$$

Instead of WO_3, other electron storing materials have also been explored such as SWNT [8], SnO_2 [9], Cu_2O [10], MoO_3 [11], and polyoxometalates [12]. However, WO_3 is the most viable and simple in construction of the hybrid materials and effective in storing the photogenerated electrons for long periods (over 12 h) [6,11,13,14] due to the conduction band (CB) level (E_{CB} = +0.41 V_{NHE}) lying positive of the oxygen reduction potential ($E(O_2/O_2^-)$ = −0.33 V_{NHE}). In addition, the TiO_2/WO_3 composites can store sufficiently large quantities of energy in terms of electric potential due to a relatively large negative flat band potential. As a result, this composite has been applied to anticorrosion of steel in corrosive environments [6,15] as well as environmental remediation [13].

Despite such great application potential, some fundamental aspects of the interfacial electron transfer between TiO_2 and WO_3 or TiO_2/WO_3 and steel remain less explored. Previous reports paid attention mostly to the maintenance period of the potential upon light off, and did not show direct evidence that the photogenerated

* Corresponding author. Tel.: +82 53 950 7371; fax: +82 53 952 1739.
E-mail address: hwp@knu.ac.kr (H. Park).

0926-3373/$ – see front matter © 2011 Elsevier B.V. All rights reserved.
doi:10.1016/j.apcatb.2011.12.006

electrons are truly transported from TiO_2 to WO_3 upon irradiation (charging cycle) and from WO_3 to steel upon light off (discharging cycle). The primary reason for a shortage of such experimental evidence may be a result of just mixing of the two components into a single composite or pasting the composite on steel. This single electrode configuration is not beneficial for gaining insight into the photoelectrochemical events in the composites. To avoid such limited access to the composite interior, the TiO_2 and WO_3 were separated into two different electrodes, galvanically coupled, and treated as a single galvanic couple in this study. In addition, TiO_2/WO_3 composite electrodes were galvanically coupled to steel in order to investigate the photogenerated electron transfers between TiO_2/WO_3 and steel electrodes. Our previous study proved that an UV-irradiated TiO_2 electrode could play the role of a non-sacrificial anode when connected to a carbon steel cathode that was placed in corrosive environments (saline water and soil) [16,17]. Despite its successful performance for corrosion prevention, the main intrinsic drawback of the TiO_2 photoanode is that the photoperformance does not last in the absence of light (i.e., at night). In this regard, combining with WO_3 is expected to prevent corrosion even in the absence of light.

2. Experimental

2.1. Electrode preparation and surface characterization

TiO_2 (Degussa P25 with a primary particle size of ca. 30 μm and BET surface area of ca. 50 $m^2\ g^{-1}$, anatase and rutile mixture of 8:2) and WO_3 (Aldrich, sub-micrometer size) mixed electrodes were fabricated by following a typical doctor-blade method [18]. TiO_2 and WO_3 mixed powders with varying weight ratios were ground with a pestle in a mortar in the presence of polyethylene glycol (PEG) solution (PEG 0.5 g L^{-1} in a mixture of ethanol and water with a volumetric ratio of 1:5), and casted onto fluorine-doped SnO_2 glass substrates (FTO, Pilkington). After drying at room temperature, the electrode was annealed at 450 °C for 30 min to remove the PEG and enhance interparticle connection. Note that TW *x* refers to the *x* weight % of TiO_2 and TW 0 means WO_3 only (e.g., TW 25 = 1 g-TiO_2/(1 g-TiO_2 + 3 g-WO_3).

Surface characterization of as-prepared TiO_2 and WO_3 electrodes was carried out with a scanning electron microscopy (SEM; Hitachi S-480). The optical properties of the electrodes were also characterized with an UV–vis diffuse reflectance spectrophotometer (Shimadzu UV2450).

2.2. Photoelectrochemical tests

TiO_2/WO_3 electrode, saturated calomel electrode (SCE), and Pt gauze were immersed in an aqueous electrolyte of 0.1 M sodium formate and 0.1 M sodium chloride (single cell, see Scheme 1a). A simulated solar light (AM 1.5, 300 mW cm^{-2}) was irradiated to the backside of TiO_2/WO_3 electrode not facing the electrolyte for a given time (light on) and then blocked (light off) from the electrode by inserting light-nontransparent film in front of the electrode. Such light on/off cycle changed the open circuit potentials (OCPs) of the electrode and the time profiles of OCPs were recorded every second with a potentiostat (EG&G 263A2). In this study, OCPs mean the difference of electrical potential between TW electrode and electrolyte in the absence or presence of irradiation. In this regard, OCPs have two meanings: equilibrium potential in the dark and photo-potential in the presence of light. When necessary, the TiO_2 electrode and WO_3 electrode were separately placed in two different cells that were connected through a salt bridge as a galvanic couple. In this case, both cells had the same electrolyte (0.1 M sodium formate and 0.1 M sodium chloride). For application to anticorrosion, TiO_2/WO_3 electrodes with varying active areas were connected to a stainless steel electrode (surface area 2.27 cm^2) as a galvanic couple, which were immersed in 0.1 M sodium formate and 0.1 M sodium chloride, respectively (Scheme 1c). A circular stainless steel (SS) electrode was mechanically polished with SiC emery paper, rinsed with acetone, and dried under nitrogen gas. The back and edges of the steel electrode were covered with epoxy resin to expose only the front surface to the electrolyte solution. In the galvanic couples, the light on/off-induced changes of the OCPs and simultaneous changes of the cell current (I_{cell}) were also recorded using the galvanic corrosion mode in the M 352 program that was supplied by EG&G. The potentiostat that runs the galvanic corrosion experiment with SoftCorr III software in effect functioned as a zero-resistance ammeter. For Nyquist plots, AC impedance measurements of the electrodes were carried out in a 1 M Na_2SO_4 solution with a frequency range of 1000–0.01 Hz with an AC voltage of 10 mV rms (Gamry Instruments REF600-03068) in the dark and under AM-1.5 light (300 mW cm^{-2}).

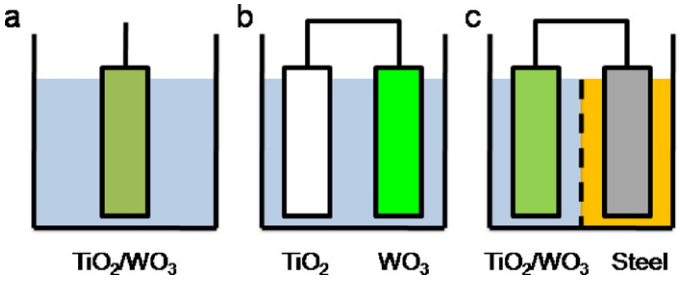

Scheme 1. Three different cell configurations. (a) TiO_2 and WO_3 mixed electrode (single working electrode) in a single cell containing a mixed electrolyte of 0.1 M sodium formate and 0.1 M sodium chloride. (b) A galvanic couple of TiO_2 electrode and WO_3 electrode in a single cell containing a mixed electrolyte of 0.1 M sodium formate and 0.1 M sodium chloride. (c) A galvanic couple of TiO_2/WO_3 electrode and steel electrode in two different cells containing 0.1 M sodium formate and 0.1 M sodium chloride, respectively.

3. Results and discussion

3.1. Characterization of semiconductor electrodes

Fig. 1 shows the SEM images of bare TiO_2 (TW 100), bare WO_3 (TW 0), and TiO_2 and WO_3 mixed (1 g-TiO_2 + 3 g-WO_3; TW 25) electrodes. The bare TiO_2 electrode consisted of fine particles of around 30 nm in size along with particle aggregation (Fig. 1a) while the bare WO_3 had larger particles of sub-micrometer size (Fig. 1b and c). When these TiO_2 and WO_3 were mixed and pasted together into a single FTO electrode, an intimate and firm contact between the two was created (Fig. 1d). Due to the respective conduction band and valence band levels of TiO_2 negative of and similar to those of WO_3, the photogenerated electrons of TiO_2 may be effectively transferred to WO_3 while the holes may be distributed to TiO_2 and WO_3 (Scheme 2). Fig. 2 displays the UV–vis absorption spectra of the mixed electrodes as a function of the TiO_2 and WO_3 weight ratio. Overall, the spectra were quite similar among them and the absorbance decreased with increasing content of WO_3 despite a larger absorption coefficient of WO_3 than TiO_2 [19]. This inconsistency may be attributed to significantly larger particles or the light-scattering effect of WO_3 compared to TiO_2 reducing the light-active surface per unit mass. Yet obviously, WO_3 exhibited an extended absorption spectrum up to around 480 nm with a bandgap of ca. 2.7 eV (extrapolated absorption onset ~455 nm).

For photoelectrochemical experiments, TiO_2 and WO_3 were physically mixed and casted onto a single FTO glass electrode as a function of the TiO_2 and WO_3 weight ratio (Scheme 1a) and linear sweep voltammograms were taken in 1 M Na_2SO_4 electrolyte.

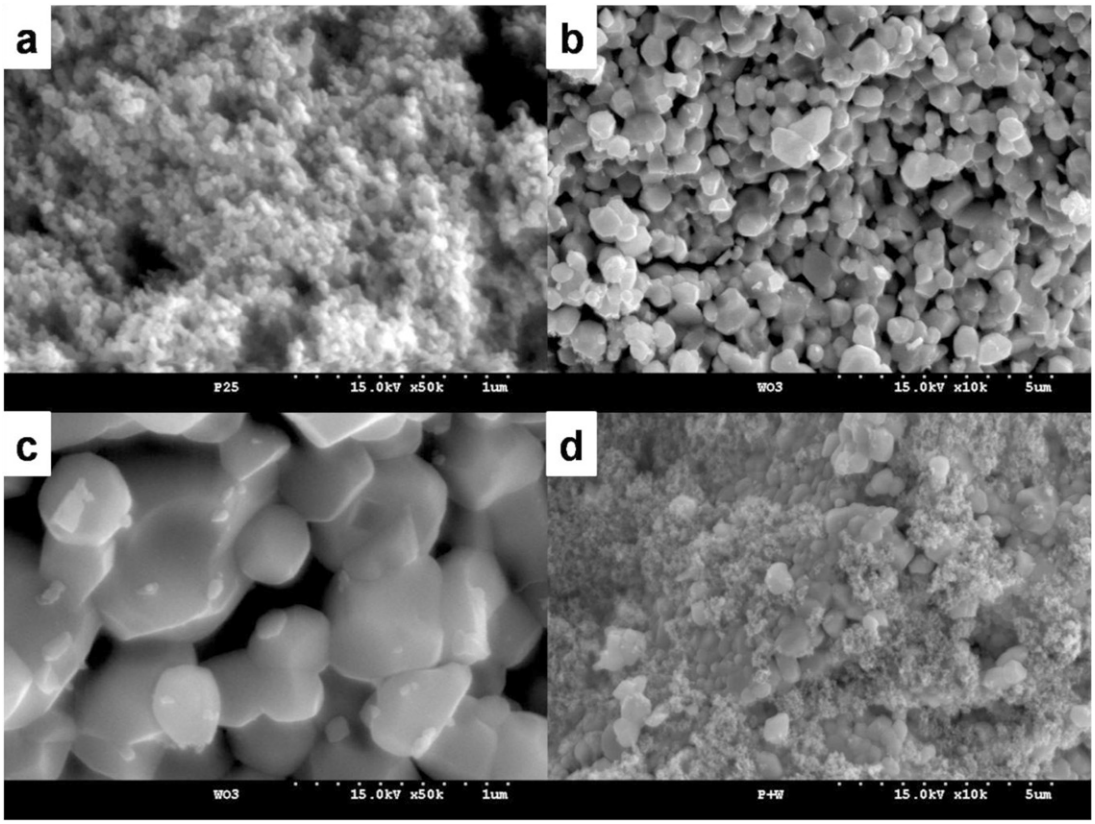

Fig. 1. SEM images of (a) bare TiO_2 (TW 100) (b and c) bare WO_3 (TW 0) and (d) TiO_2 and WO_3 mixed electrode with weight ratio of 1:3 (TW 25). TW *x* refers to *x* weight % of TiO_2 and TW 0 means bare WO_3 (e.g., TW 25 = 1 g-TiO_2/(1 g-TiO_2 + 3 g-WO_3).

As shown in Fig. 3, the bare TiO_2 (TW 100) electrode had around a 2 V wide potential window with a characteristic photocurrent peak at −1.1 V_{SCE}. This peak decreased in magnitude and simultaneously shifted to a positive potential direction as the WO_3 content increased (i.e., −1, −0.4, −0.2, and −0.1 V with TW 75, 50, 25, and 0, respectively). Similar yet less pronounced behaviors of the electrodes were also found in the dark (Fig. S1 in Supplementary Material). This indicates that those peaks may be attributed to the inherent property of the semiconductor/electrolyte interface [20] associated with adsorbed molecular oxygen [21] or surface states [22–24]. In the latter, surface states are often created by conduction band electrons during irradiation [24]. It should be pointed that the redox process related to the peaks were confined to the semiconductor surface and were not affected by mass transfer of a substance from the solution [20]. This suggests, therefore, that the anodic peaks may be associated to the charging/discharging property of the semiconductors (non-Faradaic process). The gradual shifts of the peaks to positive potential direction with increasing the WO_3 content result likely from the Fermi level of WO_3 lying positive of that of TiO_2 (see Scheme 2). When 1 M NaOH was used as an electrolyte instead of 1 M Na_2SO_4, the peaks became less obvious and significantly shifted cathodically (Fig. 3 inset) likely due to the pH-dependent shift of the flat band potentials (e.g., −59 mV pH^{-1}). This behavior was similarly found in the dark

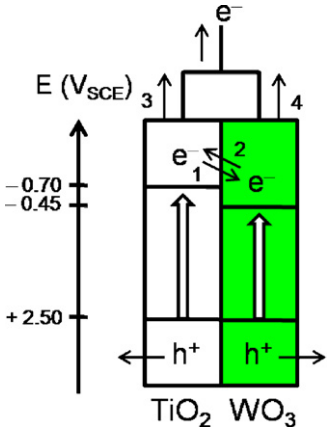

Scheme 2. Photogenerated electron transfers between TiO_2 electrode and WO_3 electrode upon light on (1 and 3) and light off (2 and 4). Note that the band positions may change depending on the synthetic ways and the particle sizes and of the semiconductors.

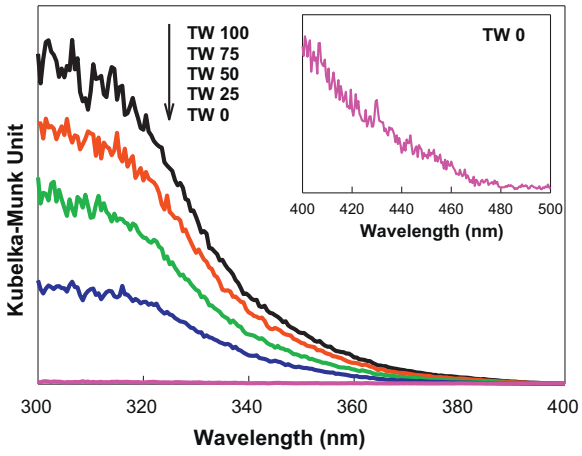

Fig. 2. UV–vis diffuse reflectance spectra of TiO_2 and WO_3 mixed electrodes with different weight ratios. Inset shows the magnified spectrum of TW 0.

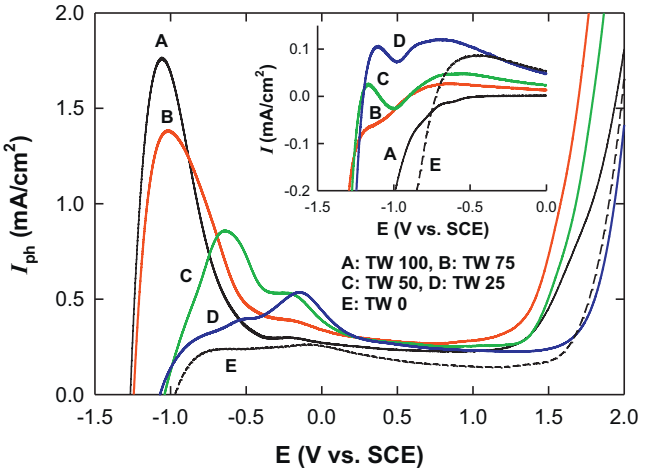

Fig. 3. Linear sweep voltammograms of TiO_2 and WO_3 mixed electrodes with different weight ratios in 0.1 M Na_2SO_4 (Inset: 0.1 M NaOH).

(Fig. S2 in Supplementary Material). Hence, they may be also associated to proton filling/removing [25]. Such proton filling/removing occurs in WO_3 as well (reactions (2) and (3)) [26] and these peaks were also seen in the voltammogram of the bare WO_3 (TW 0). The main anodic processes of the mixed electrodes appeared to initiate at 1.3 V, from which water oxidation may initiate.

Fig. 4a compares the impedance (Nyquist) plots of TiO_2 and WO_3 electrodes with different weight ratios in the frequency range between 1000 Hz and 0.01 Hz at the respective open circuit

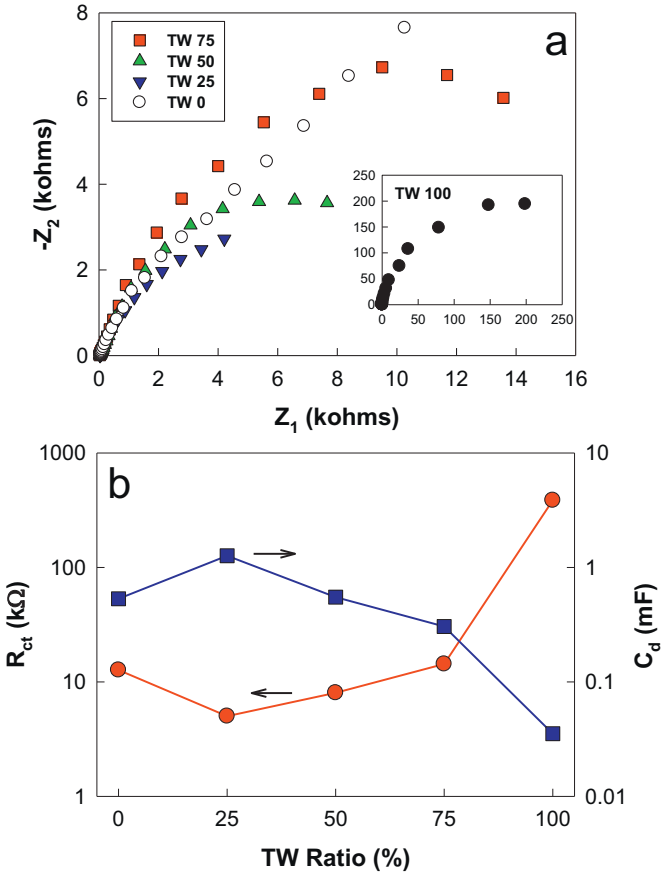

Fig. 4. (a) Impedance (Nyquist) plots of TiO_2 and WO_3 mixed electrodes with different weight ratios in 0.1 M Na_2SO_4. (b) Effects of TW ratios on the charge transfer resistance (R_{ct}) and double layer capacitance (C_d) in 0.1 M Na_2SO_4.

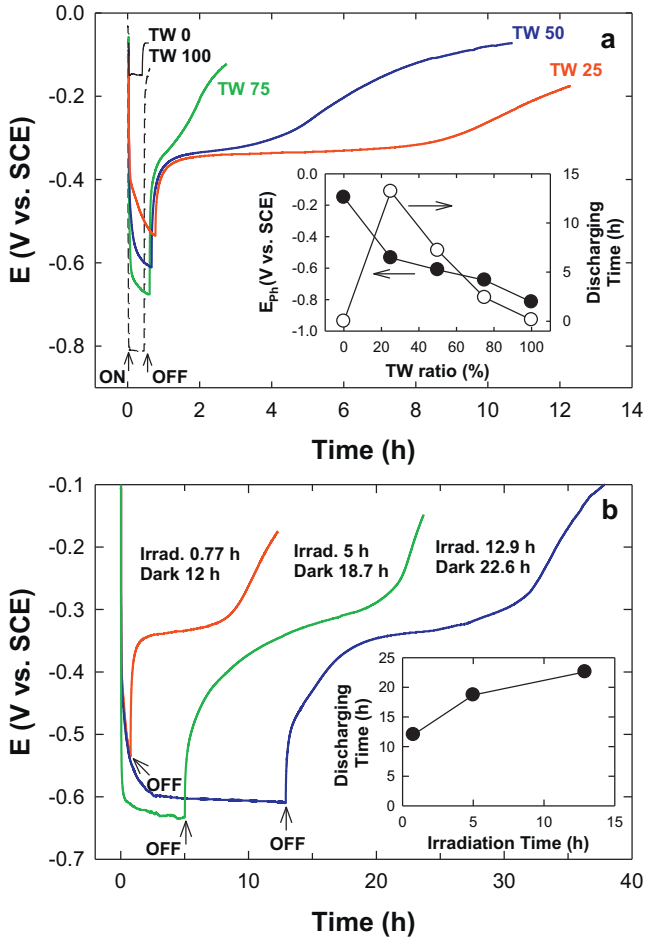

Fig. 5. Effects of (a) TiO_2 and WO_3 weight (TW) ratios and (b) irradiation periods on the changes of open circuit potentials (OCPs) and the discharging times. TiO_2 and WO_3 were fabricated into a single electrode (see Scheme 1a and TW 25 electrode was used in (b). Electrolyte: 0.1 M HCOONa + 0.1 M NaCl.

potentials. The electrochemical cell was considered to represent a simple equivalent circuit of two resistors (solution and electrode) and a single capacitor (electrode). Nyquist plots of the electrodes showed non-ideal semicircles. For example, bare WO_3 (TW 0) exhibited deviation from the semicircle at 4 kΩ of Z_{real} suggesting the existence of a mass transfer limit [27], while the other mixed electrodes seem to have additional electrical components. The detailed resolutions of the plots were beyond the scope of this study and the plots were treated as simple semicircles. The curve-fitting for the plots indicated that the bare TiO_2 (TW 100) had a very large charge transfer resistance (R_{ct}) of approximately 386 kΩ and double layer capacitance (C_d) of around 35 μF, which were varied with the WO_3 content (Fig. 4b). It should be pointed that TW 25 had the smallest value of R_{ct} with around 5 kΩ indicating that the charge transfer was most facilitated, and hence, the separation of electron-hole pairs may be significantly enhanced. In addition, TW 25 had the largest C_d value at 1.26 mF, approximately 40 and 2-fold higher than that of TW 100 and TW 0, respectively. This suggests that TW 25 may have the largest charging capacity.

3.2. *Photo-charging and discharging behaviors of the TiO_2 and WO_3 electrodes*

Fig. 5a shows the effect of the TiO_2 and WO_3 weight ratios on the OCP changes of the mixed electrodes with light on/off. When bare TiO_2 electrode (TW 100) was immersed in a mixed electrolyte of

0.1 M sodium formate and 0.1 M sodium chloride (Scheme 1a) and exposed to light (active surface area, 3.14 cm^2), its OCP immediately dropped down from ca. −0.1 V_{SCE} to ca. −0.8 V_{SCE}. However, soon after light off, it returned to the original value. In the case of the bare WO_3 electrode (TW 0), the light-induced OCP change also occurred yet the change was very small with only Δ0.1 V. In addition, similarly to TiO_2, the OCP was not maintained after light off. Hence, even though WO_3 itself is known as a photochromic material which stores electrons [28,29], the low photocatalytic activity of the WO_3 sample used in this study resulted in a very weak photochromic behavior. However, the TiO_2/WO_3 mixed electrode behaved differently either from the TiO_2 or WO_3 electrode as follows. First, the magnitude of the OCP (in terms of the absolute value) decreased with decreasing TiO_2 content. For example, TW 75 had an OCP value of ca. −0.65 V_{SCE}, which was reduced to −0.6 V_{SCE} with TW 50 and to ca. −0.55 V_{SCE} with TW 25. The gradual decrease in the OCP with decreasing TiO_2 content, therefore, indicates that the primary role of TiO_2 in the mixed electrode is to generate electron–hole pairs and provide the electrons to WO_3 (photo-charging effect). Second, the recovery time of the OCP compared to the original value (i.e., dark potential; for simplicity, it was assumed to locate at −0.15 V_{SCE}) increased with increasing amounts of WO_3. For example, the recovery times of TW 75, 50, and 25 were estimated to be ca. 2.3 h, 7.3 h, and 13 h, respectively when irradiated for 0.5 h (Fig. 5a inset). Hence the primary role of WO_3 is to store the photogenerated electrons during the period of irradiation and release them as heat (luminescence) or transfer the corresponding energy to the dissolved oxygen (formation of singlet oxygen) [30] when the irradiation was terminated. Finally, irrespective of the TW ratios (except for TW 0 and 100), it is apparent that the OCP stopped decreasing identically at around −0.37 V_{SCE} temporarily or for a certain period of time. Such pinned potentials appear to be related with the mixed Fermi levels of TiO_2 and WO_3 that are equilibrated to the redox potential of the electrolyte.

In addition to the relative weight ratio, other running conditions (e.g., irradiation time, area ratios of TiO_2 and WO_3, kinds of electrolytes and electron donor/acceptors, solution pH, etc.) may affect the overall photoelectrochemical and electrochemical behaviors of the TW electrodes. Fig. 5b shows the effect of the irradiation times for the TW 25 electrodes on their discharging times. It is obvious that prolonged irradiation increases the discharging period. A typical irradiation time of 0.77 h had a discharging period of 12 h while around 13 h-irradiation had the discharging period of 22.6 h. Interestingly, despite the correlation between the irradiation time and the discharging time, the time differences between the two were very similar with 10–13 h (Fig. 5b inset). This indicates that irradiation for 0.77 h in effect is quite sufficient to reach photocharging-discharging equilibrium and additional irradiation over 0.77 h just extends the discharging time as long as the additional irradiation time.

We have also studied the effect of the area ratios of TiO_2 and WO_3 simply by coating a semiconductor particle on each of the two separated electrodes, and connecting them galvanically and treating them as a galvanic couple (Scheme 1b). This approach is very useful in quantitatively estimating the actual currents flowing between the two semiconductor electrodes. As shown in Fig. 6, the dark potential (i.e., mixed dark potential) of the TiO_2 of 0.636 cm^2 and WO_3 of 2.269 cm^2 couple (area ratio of 1:3.56) was ca. −0.1 V_{SCE} with trace levels of current (<10^{-9} A), indicating virtually no exchange of electrons between the two. Upon irradiation, the mixed potential decreased to −0.4 V_{SCE} along with a current of +30 μA ("+" indicates that electrons flow from TiO_2 to WO_3; vice versa). When the light was off, the mixed potential rose to the original value rather quickly within an hour while the photocurrent decreased to zero in about 50 min. However, when the area ratio was increased to 1:1 (both electrodes equally 3.14 cm^2), the

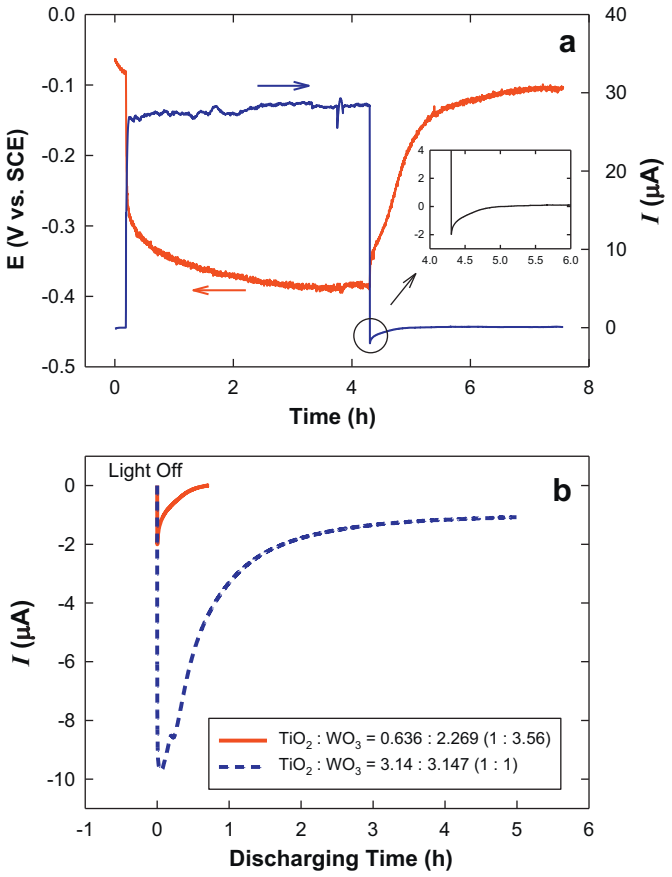

Fig. 6. (a) Time-profiled potential and simultaneous current changes of TiO_2 and WO_3 galvanic couple (area ratio of 1:3.56) upon light on and light off. (b) Time-profiled current change of TiO_2 and WO_3 galvanic couple with different area ratios of 1:3.56 and 1:1 during the discharging period after light off. Positive (+) current means the electron flow from TiO_2 to WO_3 and vice versa. Electrolyte: 0.1 M HCOONa + 0.1 M NaCl. See Scheme 1b for cell configuration.

observed dark current was at ca. −2 μA for several hours indicating that electrons flowed from WO_3 to TiO_2. Despite conduction band level of TiO_2 lying negative of WO_3 counterpart, such a reversed electron flow from WO_3 to TiO_2 may be possible due to Fermi level equilibration created via the galvanic coupling of the two.

On the basis of the above experimental results and understating on them, the overall shapes of the time-profiled OCPs (e.g., TW 25 in Fig. 5) could be divided into the following five regions. The first region is a photo-period for charge separation plus a charging period of TiO_2 (WO_3 for TW 0) occurring within a few seconds (0 V_{SCE} to −0.4 V_{SCE}) and the second is a charging period of WO_3 by the photogenerated electrons of TiO_2 that occurs slowly for several hours (mostly an hour in this study; −0.4 V_{SCE} to −0.55 V_{SCE}). The third region starts upon light off, in which the rapid discharging of TiO_2 takes place within a few seconds (−0.55 V_{SCE} to −0.37 V_{SCE}). The fourth is a stabilization period of TW electrodes, in which WO_3 stays as a reduced state for a few hours due to the slow electron transfer from WO_3 to interfacial acceptors (−0.37 V_{SCE} to −0.35 V_{SCE}). The final region is a full discharging period of TW electrodes, where all the stored electrons are transferred to the interfacial acceptors (≥−0.37 V_{SCE}).

3.3. Application to corrosion prevention of steel electrodes

For application of the TW electrodes, they were electrically connected to a SS electrode as a galvanic couple (Scheme 1c). Two different cells had different electrolytes (0.1 M sodium formate in

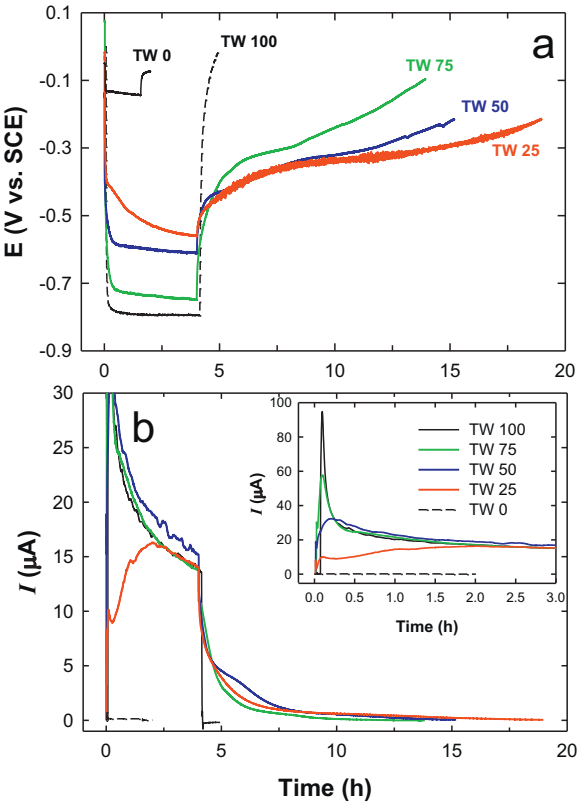

Fig. 7. Effects of TiO_2 and WO_3 weight (TW) ratios on (a) the change of open circuit potentials (OCPs) of galvanically coupled TiO_2/WO_3 electrode (0.1 M HCOONa) and steel electrode (0.1 M NaCl) through a salt bridge and (b) photocurrents and dark currents after light was off. Inset in (b) shows the full-scalled photocurrent changes with time. See Scheme 1c for cell configuration. Area ratio of TiO_2/WO_3 and steel was 1:1.

TW cell and 0.1 M NaCl in SS cell) and were connected through a salt bridge. Overall, the photoelectrochemical behaviors of the galvanic couple were similar to those of the single TW electrode (Fig. 5). TW 25 was found to be the most effective in dropping down the SS electrode to approximately $-0.55\,V_{SCE}$ under irradiation (Fig. 7a). This galvanic potential may be not sufficiently negative to theoretically protect carbon steel from corrosion (i.e., corrosion immunity region of Fe^0 $\sim -0.77\,V_{SCE}$) due to a very severe corrosive environment (0.1 M NaCl). Yet, stainless steel is intrinsically corrosion-resistant and may be protected from corrosion. Other TW series electrodes also may delay the corrosion progress of SS and increase its service lifetime. When light was off, TW electrodes (except TW 0) supplied the photogenerated electrons to SS at I_{cell} of 0.1–1 μA continuously over several hours (Fig. 7b). The electrons flowing into the SS may be scavenged by dissolved oxygen, forming hydrogen peroxide [17]. Since hydrogen peroxide could be detrimental to stainless steel, the number of electrons flowing should be minimized or kept stored at the TW electrode for achieving sufficiently negative electric potentials of the SS. Finally, the area ratios of the TW and SS were changed and their effects on the magnitudes of E_{mix} and I_{cell} were investigated. As shown in Fig. 8, a ratio of 0.28:1 resulted in an E_{mix} of $-0.35\,V_{SCE}$ and I_{cell} of ~2 μA (Fig. 8 inset) yet was found to be ineffective in storing the electrons under 4 h of irradiation. The charging/discharging effect was shown with a ratio 1:1 and 1.38:1. Upon light on, their mixed potentials ($-0.55\,V_{SCE}$) and the corresponding magnitude of the photocurrents (~15 μA) were quite similar between the two area ratios. However, the 1:1 ratio had a relatively short discharging period with ca. 5 h while the discharging period of the 1.38:1 ratio was maintained for over 20 h. Hence, in order to ensure a long period of discharging effect in the

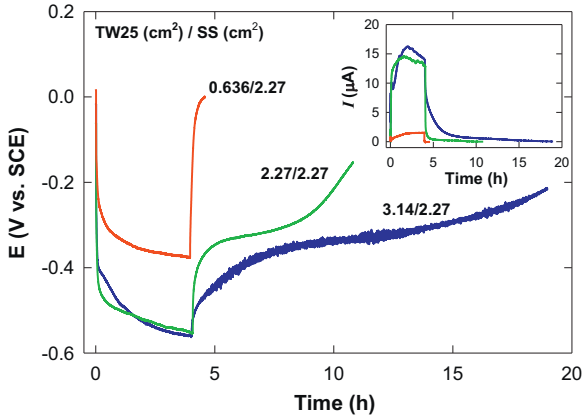

Fig. 8. Time-profiled open circuit potential (OCP) and simultaneous current changes (inset) of TiO_2/WO_3 (TW 25) and steel galvanic couple with different area ratios upon light on and light off. Electrolytes and cell configuration were identical to those in Fig. 6.

TW and SS couple or when TW is coated on a SS surface, the area of the TW should be larger than the SS but not necessarily too large.

4. Conclusions

This study showed that TiO_2 and WO_3 mixed electrodes function by storing photon energy as a form of electricity. For such a function, TiO_2 effectively worked as a light-harvesting electrode while WO_3 worked as an energy-storing electrode. Under irradiation, WO_3 was charged by the photogenerated electrons of TiO_2 and discharged for a much longer period than the irradiation period with reversed electron flow upon light off. The charging capacity or discharging period was affected by the irradiation time and by the ratios between TiO_2 and WO_3 in weight and area. Application of TiO_2 and WO_3 mixed electrodes to anticorrosion also demonstrated that the mixed electrodes could provide the photogenerated electrons overflowed from WO_3 to the galvanically coupled steel via a potential cascade of $TiO_2 \rightarrow WO_3 \rightarrow$ steel (during irradiation) and $WO_3 \rightarrow$ steel upon light off.

Acknowledgements

This research was supported by the Basic Science Research Programs (no. 2009-0071350, 2009-0089904, 2010-0002674, and 2011-0021148) and by the Korea Center for Artificial Photosynthesis (NRF-2009-C1AAA001-2009-0093879) through the National Research Foundation of Korea (NRF) funded by the Ministry of Education, Science and Technology.

Appendix A. Supplementary data

Supplementary data associated with this article can be found, in the online version, at doi:10.1016/j.apcatb.2011.12.006.

References

[1] N.S. Lewis, D.G. Nocera, Proc. Natl. Acad. Sci. 103 (2006) 15729–15735.
[2] D. Ginley, M.A. Green, R. Collins, MRS Bull. 23 (2008) 355–364.
[3] H. Ibraim, A. Ilinca, J. Perroh, Renew. Sustain. Energy Rev. 12 (2008) 1221–1250.
[4] N.A. Campbell, J.B. Reece, L.A. Urry, M.L. Cain, S.A. Wasserman, P.V. Minorsky, R.B. Jackson, Biology, 8th ed., Pearson, San Francisco, 2008.
[5] Basic research needs for solar energy utilization, U.S. Department of Energy, available on the web at http://www.sc.doe.gov/bes/reports/files/SEU_rpt.pdf, 2005.
[6] T. Tatsuma, S. Saitoh, Y. Ohko, A. Fujishima, Chem. Mater. 13 (2001) 2838–2842.
[7] T. Tatsuma, S. Saitoh, P. Ngaotrakanwiwat, Y. Ohko, A. Fujishima, Langmuir 18 (2002) 7777–7779.
[8] A. Kongkanand, P.V. Kamat, ACS Nano 1 (2007) 13–21.

[9] R. Subasri, T. Shinohara, Electrochem. Commun. 5 (2003) 897–902.
[10] J.P. Yasomanee, J. Bandara, Sol. Energy Mater. Sol. Cells 92 (2008) 348–352.
[11] Y. Takahashi, P. Ngaotrakanwiwat, T. Tatsuma, Electrochim. Acta 49 (2004) 2025–2029.
[12] P. Ngaotrakanwiwat, S. Saitoh, Y. Ohko, T. Tatsuma, A. Fujishima, J. Electrochem. Soc. 150 (2003) A1405–A1407.
[13] D. Zhao, C. Chen, C. Yu, W. Ma, J. Zhao, J. Phys. Chem. C 113 (2009) 13160–13165.
[14] S. Higashimoto, M. Sakiyama, M. Azuma, Thin Solid Films 503 (2006) 201–206.
[15] Z.L. Jin, X.J. Zhang, Y.X. Li, S.B. Li, G.X. Lu, Catal. Commun. 8 (2007) 1267–1273.
[16] H. Park, K.Y. Kim, W. Choi, Chem. Commun. (2001) 281–282.
[17] H. Park, K.Y. Kim, W. Choi, J. Phys. Chem. B 106 (2002) 4775–4781.
[18] H. Park, E. Bae, J.-J. Lee, J. Park, W. Choi, J. Phys. Chem. B 110 (2006) 8740–8749.
[19] P.S. Patil, S.H. Mujawar, A.I. Inamdar, P.S. Shinde, H.P. Deshmukh, S.B. Sadale, Appl. Surf. Sci. 252 (2005) 1643–1650.
[20] H.O. Finklea (Ed.), Semiconductor Electrodes, Elsevier, New York, 1988.
[21] B. Parkinson, F. Decker, J.F. Juliao, M. Abramovich, H.C. Chagas, Electrochim. Acta 25 (1980) 521–525.
[22] C. Gutierrez, P. Salvador, J. Electroanal. Chem. 138 (1982) 457–463.
[23] P. Salvador, C. Gutierrez, Chem. Phys. Lett. 86 (1982) 131–134.
[24] R.H. Wilson, J. Electrochem. Soc. 127 (1980) 228–234.
[25] M.F. Weber, L.C. Schumacher, M.J. Dignam, J. Electrochem. Soc. 129 (1982) 2022–2028.
[26] J.P. Randin, A.K. Vijh, A.B. Chughtai, J. Electrochem. Soc. 120 (1973) 1174–1184.
[27] A.J. Bard, L.R. Faulkner, Electrochemical Methods: Fundamentals and Applications, 2nd ed., Wiley, New York, 2001.
[28] P.M.S. Monk, Crit. Rev. Solid State Mater. Sci. 24 (1999) 193–226.
[29] C.G. Granqvist, Sol. Energy Mater. Sol. Cells 60 (2000) 201–262.
[30] J. Kim, C.W. Lee, W. Choi, Environ. Sci. Technol. 44 (2010) 6849–6854.